New Developments and Challenges in Remote Sensing, Z. Bochenek (ed.)


# A genetic approach to Pan-sharpening of multispectral images

A. Garzelli & F. Nencini
*Department of Information Engineering, University of Siena, Siena, Italy*

Keywords: image fusion, Pan-sharpening, genetic algorithms

ABSTRACT: This paper presents a novel image fusion method, suitable for sharpening of multispectral (MS) images by means of a panchromatic (Pan) observation, based on a modified generalized intensity-hue-saturation algorithm: the MS bands expanded to the finer scale of the Pan image are sharpened by adding the spatial details derived from a difference image, which is calculated by the Pan image and a linear combination of the MS bands. Since a direct, unconditioned injection of Pan details gives unsatisfactory results, a new injection model is proposed, which provides the optimum injection by maximizing a global quality index of the fused product. The optimum injection is driven by an index function capable to measure radiometric, geometric and spectral distortions in the fused images. Fusion tests are carried out both on spatially degraded data to objectively compare the proposed scheme to the most promising state-of-the-art image fusion methods (included two commercial software solutions), and on full resolution image data to visually assess the performance of the proposed genetic image fusion method.

## 1 INTRODUCTION

Spaceborne imaging sensors allow a global coverage of the Earth surface to be achieved on a routine basis. Multispectral (MS) observations, however, exhibit ground resolutions that may be inadequate to specific identification tasks especially when urban areas are concerned. After the successful launch of the new generation of satellite imagers, e.g., Ikonos, QuickBird, and SPOT-5, very high-resolution MS and panchromatic (Pan) images are made available.

Data fusion techniques, originally devised to allow integration of different information sources, may take advantage of the complementary spatial/spectral resolution characteristics for producing spatially enhanced MS observations. This specific aspect of data fusion is often referred to as data merge (Scheunders 2001) or band-sharpening (Kumar *et al*. 2000). More specifically, Pan-sharpened MS is a fusion product in which the MS bands are sharpened via the higher-resolution Pan image. In fact, the latter is acquired with the maximum resolution allowed by the imaging sensor, as well as by the datalink throughput, while the former are acquired with coarser resolutions, typically, two or four times lower, because of SNR constraints and transmission bottleneck. After being received at ground stations, the Pan image may be merged with the MS data to enhance their spatial resolution.

The description of the proposed fusion algorithm is organized as follows. Section 2 deals with the image analysis tools used in the proposed Pan-sharpening algorithm with

emphasis on the structure of the sharpening model and the quality evaluation criterion. In section 3 a general GA scheme is described, based on floating point representation of chromosomes and on genetic operators borrowed from the most promising studies on genetic algorithms (GA). How the GA is used to regulate the Pan injection is explained in section 4. Experimental results and comparisons are presented and discussed in section 5 on Quickbird data set. Conclusions are drawn in section 6.

## 2 IMAGE ANALYSIS

### 2.1 *Structure of the Pan-sharpening model*

The definition of a suitable model for the injection of Pan details is a crucial point for a good quality of the data fusion product. The most promising methods have developed different models, generally related to a common approach that consists of calculating the parameters that regulate the injection (typically gain and offset) at a coarser resolution and then adopting those parameters to the finer resolution. This means that the scale persistence is exploited supposing that the characteristics of edges and texture at coarser scales are not too much different from the finer scales. This hypothesis is verified if the ratio between the spatial resolutions of MS and Pan data is not too high and if the model is opportunely defined. Some successful techniques, Spectral Distortion Minimization (SDM) (Alparone *et al*. 2003), Context Based Decision (CBD) (Aiazzi *et al*. 2002), Ranchin-Wald-Mangolini method (RWM) (Ranchin *et al*. 2003), have developed interesting models in which the Pan injection is regulated by the ratio between the standard deviations of the MS and Pan data, or by the first moment of inertia.

The problem that generally occurs when applying those fusion techniques is that the definition of the model parameters does not correspond to an optimum choice in terms of geometric, radiometric and spectral distortions of the fused product. Besides, the definition of a local model often gives rise to numerical instability and unsatisfactory visual quality throughout the image.

The proposed Pan-sharpening algorithm applies a Generalized Intensity-Hue-Saturation (GIHS) transformation to the MS bands, (Chibani 2002). The GIHS is a linear transform which yields the generalized intensity GI

$$GI = \sum_{l=l}^{N} \alpha_l \widetilde{MS}_l \tag{1}$$

with $\widetilde{MS}_l$ denoting the expanded MS images. Only the GI component is used to extract the high-frequency spatial details from the Pan image:

$$D = P - GI \tag{2}$$

with P the Pan image.

The injection model is a simple linear model in which the coefficients that equalize the Pan image are derived globally – one for each band- from coarser scales, similarly to previous schemes such as SDM, CBD and RWM, but not *a-priori* defined on image

statistics, e.g., variance, mean, correlation coefficient, etc. The fused $l$-th MS band is computed as

$$\widehat{MS}_l = \widetilde{MS}_l + g_l \cdot D \tag{3}$$

and a genetic algorithm is applied to determine the $\alpha_l$ coefficients of eq.(1) and the $g_l$ gains of eq.(3) that maximize an image quality score index described in the next subsection.

The goal of the GA is to find the best combination of the 2N real coefficients $\alpha_l$ and $g_l, l = 1, \ldots N$, according to an objective criterion that describes the enhancement of the MS images. The representation of the GA chromosomes is therefore a string of 2N real numbers (8 coefficients in the case of QuickBird image data set). The representation of the chromosomes is therefore a string of real numbers as reported in eq.(4).

$$\textit{Chromosome } \mathbf{c}\text{:}\{g_1, g_2, g_3, \cdot, \cdot, \cdot, g_N, \alpha_1, \alpha_2, \alpha_3, \cdot, \cdot, \cdot, \alpha_N\} \tag{4}$$

### 2.2 *Quality evaluation criterion*

The image quality index $Q4$ for multispectral images having four spectral bands can be calculated on Pan-sharpened MS images as described in (Alparone *et al*. 2004). The index $Q4$ is derived from the theory of hypercomplex numbers, in particular of ''quaternions'', which can be represented in the form $\mathrm{a} = a_1 + a_2\, i + a_3 j + a_4\, k$, where $a_1$, $a_2$, $a_3$, $a_4$ are real numbers, and $i^2 = j^2 = k^2 = i\, j\, k = -1$. For MS images with four spectral bands, typical for new generation satellite images, $a_1,\ a_2,\ a_3,\ a_4$ represent the values assumed by a given image pixel in the four bands, acquired in the Blue, Green, Red and Near Infrared wavelengths.

The unique score index $Q4$ for 4-band MS images, which assumes a real value in the interval [0,1], is a generalization of the Q index defined in (Wang 2002) and is equal to 1 iff the MS image is identical to the reference image. $Q4$ is made up of different components (factors) to take into account for the correlation, the mean of each spectral band, the intra-band local variance, and the spectral angle. The first three factors are also taken into account by Wang & Bovik's index (Q) for each band while the spectral angle is introduced by $Q4$ by properly defining a $CC$ of multivariate data. In this way, both radiometric and spectral distortions are considered by a single parameter.

The more $Q4$ approaches to unity, the higher becomes the radiometric and spectral quality of the fused image. This suggests that this index can be used not only to evaluate the performances of fusion algorithms, but also as a target function to be maximized in order to compute optimal fusion parameters.

## 3 GENETIC COMPONENTS

Genetic algorithms (Davis 1991; Michalewicz 1994) are inspired by the evolution of populations. In a particular environment, individuals which fit the environment better will be able to survive and hand down chromosomes to their descendants, while less fit individuals will become extinct. The aim of genetic algorithms is to use simple representations to encode complex structures and simple operations to improve these

structures. Therefore, genetic algorithms are characterized by their representations and operators. A fitness function is defined which measures the fitness of each individual. The populations are evolved to find good individuals as measured by the fitness function. A GA flow diagram is shown in figure 1(a), and each of the major components is discussed in the following sections. A GA requires the definition of these fundamental steps: chromosome representation, selection of a function also called fitness function, creation of the initial population, reproduction function, mutation and crossover operators, termination criteria, and the evaluation of fitness function. The following subsections describe these issues.

### 3.1 *Chromosome representation*

A chromosome representation is necessary to describe each individual in the GA population. The representation scheme determines how the problem is structured in the GA and also determines the genetic operators that are used. Each chromosome is made up of a sequence of genes from a predefined alphabet. One useful representation of chromosome for function optimization involves genes from an alphabet of floating point numbers with values limited by an upper and a lower bound. It has been shown by Michalewicz (Michalewicz 1994) that a real-valued GA is more efficient in terms of *CPU time* and more accurate in terms of precisions for replications than binary GA representations.

### 3.2 *Reproduction*

An important role in GA's is the selection of individuals to produce successive generations usually called reproduction. A probabilistic selection is performed based upon the individual's fitness such that the better individuals have an increased chance of being selected. An individual in the population can be selected more than once with all individuals in the population having a chance of being selected to reproduce into the next generation.

Ranking methods, which produce best performances, require the evaluation function to map the solutions to a partially ordered set and assign a probability of selection, $P_i$, based on the rank of solution $i$ when all solutions are sorted. Normalized geometric ranking defines $P_i$ for each individual by:

$$P_i = \frac{q(1-q)^{r-1}}{1-(1-q)^{PopSize}} \tag{5}$$

where $q$ is the probability of selecting the best individual, *PopSize* is the overall number of chromosomes and r is the rank of the individual, where 1 is the best.

### 3.3 *Genetic operators*

Genetic operators provide the basic search mechanism of the GA. The operators are used to create new solutions based on existing solutions in the population. There are two basic types of operators: *crossover* and *mutation.* Operators for real-valued representations, i.e., an alphabet of floats, were developed in (Michalewicz 1994). Crossover takes two

individuals and produces two new individuals while mutation alters one individual to produce a single new solution. The application of these two basic types of operators and their derivatives depends on the chromosome representation used. For real $\overline{X}$ and $\overline{Y}$ m-dimensional vectors representing chromosomes, the following operators are defined: uniform mutation, non-uniform mutation, multi-non-uniform mutation, boundary mutation, simple crossover, arithmetic crossover, and heuristic crossover. Let $a_i$ and $b_i$ be the lower and upper bound, respectively, for each variable *i.*

3.3.1 *Mutation*

Uniform mutation randomly selects one variable, *j,* and sets it equal to a uniform random number bounded by $a_i$ and $b_i$ terms:

$$x_i' \begin{cases} U(a_i, b_i) & \text{if } i = j \\ x_i & \text{otherwise} \end{cases} \tag{6}$$

Boundary mutation randomly selects one variable, *j,* and sets it equal to either its lower or upper bound, where $r = U\ (0,1)$:

$$x_i' = \begin{cases} a_i & \text{if } i = j, r < 0.5 \\ b_i & \text{if } i = j, r \geq 0.5 \\ x_i & = \text{otherwise} \end{cases} \tag{7}$$

Non-uniform mutation randomly selects one variable, j, and sets it equal to a non-uniform random number:

$$x_i' = \begin{cases} x_i + (b_i - x_i)\left(r_2\left(1 - \frac{G}{G_{\max}}\right)\right)^b if\ r_1 < 0.5 \\ x_i - (x_i + a_i)\left(r_2\left(1 - \frac{G}{G_{\max}}\right)\right)^b if\ r_1 \geq 0.5 \\ x_i \quad otherwise \end{cases} \tag{8}$$

where $r_1$ and $r_2$ are uniform random numbers between (0,1), $G$ and $G_{max}$ are respectively the current and the maximum number of generations, $b$ is a shape parameter.
The multi-non-uniform mutation operator applies the non-uniform operator to all of the variables in the parent $\overline{X}$.

3.3.2 *Crossover*

Real-valued simple crossover generates a random number $r$ from a uniform distribution from 1 to $m$ and creates two new individuals ($\overline{X}'$ and $\overline{Y}'$) according to equation (9).

$$x_i'(y_i') = \begin{cases} x_i(y_i) & \text{if } i < r \\ y_i(x_i) & \text{otherwise} \end{cases} \tag{9}$$

Arithmetic crossover produces two complimentary linear combinations of the parents, where $r = U(0, 1)$:

$$\overline{X}' = r\overline{X} + (1 - r)\overline{Y} \tag{10}$$

$$\overline{Y}' = (1 - r)\overline{X} + r\overline{Y} \tag{11}$$

Heuristic crossover produces a linear extrapolation of the two individuals. This is the only operator that utilizes fitness information. A new individual is created when $\overline{X}$ is better than $\overline{Y}$ in terms of fitness. If the new individual is infeasible, *i.e.,* there is at least a new gene smaller than $a_i$ or bigger than $b_i$, then generate a new random number $r$ and create a new solution. After $t$ failures, the process is not repeated and the children is set equal to parents.

### 3.4 *Initialization, termination and fitness function*

To start the search of the optimal solution by GA is necessary to provide an initial population as indicated in figure 1(a). The most common method is to randomly generate solutions for the entire population. The GA moves from generation to generation selecting and reproducing parents until a termination criterion is met. A maximum number of generations is commonly used to stop the GA search. Another termination strategy involves population convergence criteria. Evaluation functions of many forms can be used in a GA, subject to the minimal requirement that the function can map the population into a partially ordered set. As stated in section (2.2), the evaluation function to be optimized is *Q4* which is particulary suited for minimizing radiometric and spectral distortions.

### 3.5 *Summary*

The GA parameters selected for the optimization of *Q*4 are listed in table 1.

The interval of variation for the $g_i$ and $\alpha_i$ parameters is the same for all bands and spans in the interval [−10,10] and [0,10] respectively, in order to ensure a wide state space. Each unknown parameter is spatially constant on the corresponding band *i*.

Table 1. GA parameters used for real-valued Q4 function optimization.

| Operation | Parameters |
|---|---|
| Initial Population | 200 |
| Normalized Geometric Selection | 0.05 |
| Uniform Mutation | 4 |
| Non-Uniform Mutation | [4, 100, 3] |
| Multi-Non-Uniform Mutation | [6, 100, 3] |
| Boundary Mutation | 4 |
| Simple Crossover | 2 |
| Arithmetic Crossover | 2 |
| Heuristic Crossover | [2, 3] |
| Maximum Generation | 200 |
| Chromosomes Bounds (for each band) | $g_i$ : [−10, 10] $\alpha_i$ : [0, 10] |

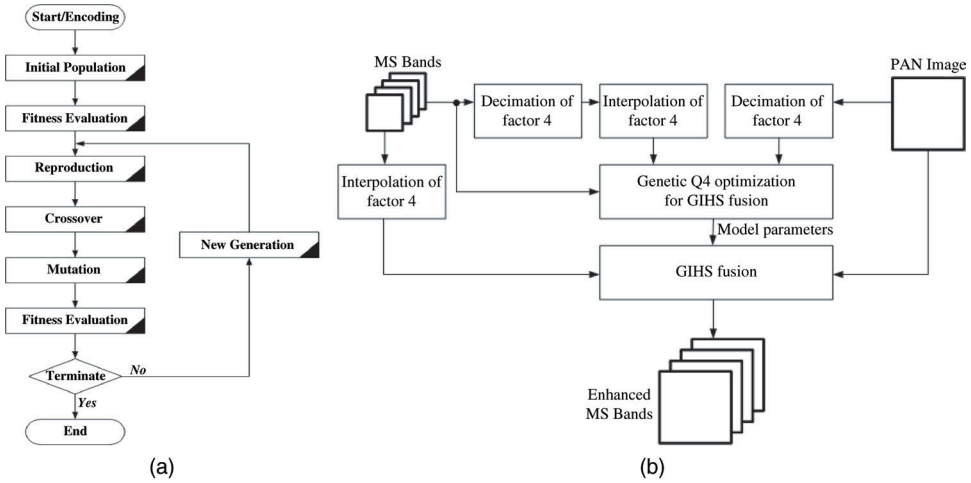


Figure 1. (a) Flow diagram of GA; (b) Flowchart of Pan-sharpening based on GA with 1 : 4 scale ratio.

## 4 DATA FUSION

Figure 1(b) outlines a procedure suitable for fusion of MS and Pan image data whose scale ratio is 4. Before the injection process, the MS images are interpolated by 4 along rows and columns, in order to process MS images having the same spatial scale of the Pan image. The interpolator and decimator blocks are implemented applying twice the *upsampling*and *downsampling* operators.

To drive the injection of Pan data, the eq.(1), (2) and (3) are applied, with c representing the best chromosome derived by the GA search. The $Q4$ index, which is capable to measure distortions but requires as inputs the fused and the reference MS images, is calculated at coarser resolution, *i.e.,* at a resolution degraded by a factor equal to 4. The GA, simulating the injection process at a degraded scale, is finally applied with the parameters described in table 1.

## 5 EXPERIMENTAL RESULTS AND COMPARISONS

The proposed fusion procedures have been assessed on two very high-resolution image data sets collected by Quickbird spaceborne MS scanner. The former is acquired on the urban area of Rome. The four MS bands span the visible and near infrared (NIR) wavelengths and are spectrally disjointed: blue $(\mathrm{B1} = 450 \div 520\,\mathrm{nm})$, green $(\mathrm{B2} = 520 \div 600\,\mathrm{nm})$, red $(\mathrm{B3} = 630 \div 690\ \mathrm{nm})$, and NIR $(\mathrm{B4} = 760 \div 900\,\mathrm{nm})$. The PAN band embraces the whole interval $(\mathrm{Pan} = 450 \div 900\,\mathrm{nm})$. All the data have been radiometrically calibrated from digital counts, orthorectified, i.e., resampled to uniform ground resolutions of 2.8m and 0.7 m for MS and PAN, respectively, and packed in 16-bit words. The original PAN image is of size $1024 \times 1024$ and the original MS data set is of size $256 \times 256$.

A thorough performance comparison was carried out among the novel method and the following state-of-the-art image fusion methods:

1. *Generalized Intensity Hue Saturation* (GIHS) (Carper *et al*. 1990);
2. *Synthetic Variable Ratio* (SVR) (Carper *et al*. 1990);
3. *Additive Wavelet Transform* (AWL) as proposed by Nunez *et al*. in (Nunez *et al*. 1999);
4. *Ranchin-Wald-Mangolini Method* (RWM) as described in (Ranchin *et al*. 2003);
5. *Context-Based Decision Method* (CBD) (Aiazzi *et al*. 2002);
6. *Gram-Schmidt spectral sharpening method* (GS) (Laben 2000) as implemented in ENVI®;
7. *Zhang Method* (ZM) (Zhang 2002) as implemented in PCI Geomatica®.

To this purpose, the datasets have been spatially degraded by four, according to Wald's protocol (Wald *et al*. 1997), and statistics have been calculated between fused and original data.

Score band-independent indexes, which are used to evaluate performances of fusion methods, are ERGAS (Ranchin *et al*. 2003), Spectral Angle Mapper (SAM) (Alparone *et al*. 2003) and Q4 index as described in subsection 2.2. The values of the three indexes are calculated for each fusion method and are reported in table 2 for 4 : 1 fusion carried out on spatially degraded data. The results show that GA fusion outperforms the other fusion methods for all three indexes. A performance ranking of algorithms indicates that the GA method is followed by ZM, RWM, CBD and GS methods whose performances highly depend on the particular data set being considered.

Figure 2 reports $128 \times 128$ tiles of the expanded images and the GA, GIHS fused data at $0.7m$. In all figures, true color (B2-B1-B0) composites, instead of false color (B3-B2-B1) composites are shown because fusion methods typically fail on the blue band (B0). Figure 2(b) demonstrates that Pan accurately sharpens and does not over-enhance the MS images. Finally, a comparison between fused and lower-scale original images shows that evident spectral distortions are totally avoided by proposed algorithm but not by GIHS method.

Table 2. ERGAS, SAM, Q4 indexes between 2.8 m MS bands and 11.2 m MS bands merged with 2.8 m Pan.

| | EXP | GA | IHS | SVR | AWL | RWM | CBD | GS | ZM |
|---|---|---|---|---|---|---|---|---|---|
| ERGAS | 4.907 | 3.022 | 3.767 | 3.744 | 3.589 | 3.376 | 3.366 | 3.468 | 3.257 |
| SAM | 4.050 | 3.471 | 4.519 | 4.050 | 5.244 | 3.747 | 3.735 | 3.715 | 3.649 |
| Q4 | 0.791 | 0.937 | 0.901 | 0.899 | 0.905 | 0.919 | 0.917 | 0.911 | 0.917 |

## 6 CONCLUSIONS

In this article it has been shown that the proposed method based on a genetic algorithm is better suited for accurate spectral preserving image merging than the most efficient

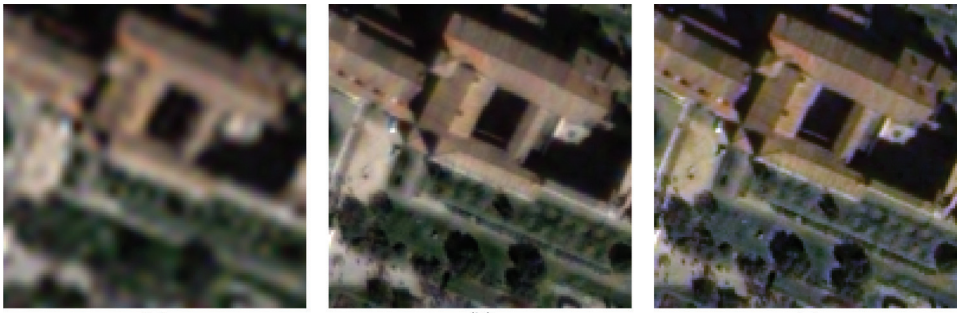


Figure 2. Examples of full-scale spatial enhancement of fusion algorithms displayed as $128 \times 128$ true color compositions at 0.7 m pixels spacing of Roma data set. (a): original MS bands (2.8 m) resampled to the scale of Pan image (0.7 m); (b): GA fusion product; (c): GIHS fusion product.

state-of-the-art fusion techniques. In particular, the injection process of the proposed algorithm based on a modified version of the GIHS method outperforms the well-known wavelet-based methods and the best commercial software solutions. Experiments carried out on very high resolution Quickbird images have shown that the proposed algorithm is quantitatively more efficient than other image fusion methods. Moreover the algorithm is capable of enhancing the spatial quality while preserving the spectral content of the MS image data regardless of whether the observed scenario is urban, or forestal, or agricultural.

## REFERENCES

Aiazzi, B., Alparone, L., Baronti, S., and Garzelli, A. 2002. Context-driven fusion of high spatial and spectral resolution data based on oversampled multiresolution analysis. *IEEE Trans. Geosci. Remote Sensings 40(10),* 2300–2312.

Alparone, L., Aiazzi, B., Baronti, S., and Garzelli, A. 2003. Sharpening of very high resolution images with spectral distortion minimization. In *Proc. IEEE Int. Geoscience And Remote Sensing Symposium,* pp. 21–25.

Alparone, L., Baronti, S., Garzelli, A., and Nencini, F. 2004. A global quality measurement of pan-sharpened multispectral imagery. *IEEE Geosci. Remote Sensing Lett. 1(4),* 313–317.

Carper, W., Lillesand, T., and Kiefer, R. 1990. The use of intensity-hue-saturation transformations for merging spot panchromatic and multispectral image data. *Photogram. Eng. Remote Sensing 56(4),* 459–467.

Chibani, Y. and Houacine, A. 2002. The joint use of IHS transform and redundant wavelet decomposition for fusing multispectral and panchromatic images. *Int. J. Remote Sensing* 23(18), 3821–3833.

Davis, L. 1991. *The Handbook of Genetic Algorithms.* Van Nostran Reingold, New York.

Kumar, A.S., Kartikeyan, B., and Majumdar, K.L. (2000). Band sharpening of IRS-multispectral imagery by cubic spline wavelets. *Int. J. Remote Sensing 21(3),* 581–594.

Laben, C.A. and Brower, B.V. 2000. *Process for enhancing the spatial resolution of multispectral imagery using pan-sharpening.* Eastman Kodak Company, Tech. Rep. US Patent #6,011,875.

Michalewicz, Z. 1994. *Genetic Algorithms+Data Structures.* Evolution Programs, Springer-Verlang, New York.

Núñez, J., Otazu, X., Fors, O., Prades, A., Palà, V., and Arbiol, R. (1999). Multiresolution-based image fusion with additive wavelet decomposition. *IEEE Transactions on Geoscience and Remote Sensing* 37(3), 1204–1211.

Ranchin, T., Aiazzi, B., Alparone, L., Baronti, S., and Wald, L 2003. Image fusion-the arsis concept and some successful implementation schemes. In *ISPRSJ. Photogramm. Remote Sensing,* Volume 58, pp. 4–18.

Scheunders, P. and Backer, S. D. (2001). Fusion and merging of multispectral images with use of multiscale fundamental forms. *J. Opt. Soc. Am. A 18(10),* 2468–2477.

Wald, L., Ranchin, T., and Mangolini, M. 1997. Fusion of satellite images of different spatial resolutions: assessing the quality of resulting images. *Photogramm. Eng. Remote Sens. 63(6),* 691–699.

Wang, Z. and Bovik, A.C. 2002. A universal image quality index. *IEEE Signal Processing Lett. 9(3),* 81–84.

Zhang, Y. 2002. A new automatic approach for effectively fusing landsat 7 images and ikonos images. In *Proc. IEEE Int. Geoscience And Remote Sensing Symposium,* pp. 2429–2431.